Applied Energy 90 (2012) 233–240

Contents lists available at ScienceDirect

Applied Energy

journal homepage: www.elsevier.com/locate/apenergy

Optimum design of shading-type building-integrated photovoltaic claddings with different surface azimuth angles

Liangliang Sun *, Lin Lu, Hongxing Yang

Renewable Energy Research Group (RERG), Department of Building Services Engineering, The Hong Kong Polytechnic University, Kowloon, Hong Kong, China

ARTICLE INFO

Article history:
Received 9 September 2010
Received in revised form 21 January 2011
Accepted 27 January 2011
Available online 25 February 2011

Keywords:
Shading-type building-integrated photovoltaic cladding
BIPV
Optimum design
Energy saving
Surface azimuth angle

ABSTRACT

The shading-type BIPV claddings can act as power generators as well as external shading devices and insulation panels. There is little available information about the impacts of orientations and inclinations on the combined energy effects of the shading-type BIPV claddings, including the power output of PV modules, the cooling load reduction of windows and concrete walls. It is worth studying the effects of different shading-type BIPV cladding designs on the total energy saving in order to maximize the system's energy performance. By considering the meteorological conditions in Hong Kong, the energy effect of the shading-type BIPV claddings with different surface azimuth angles, in terms of electricity generation and cooling energy consumption reduction is analyzed in this paper. Based on the investigations, the optimum design of the shading-type BIPV claddings for different orientations can be achieved.

1. Introduction

Many policy makers and developers have tried to reduce the greenhouse gas emission and the drastic increases in oil prices by promoting the applications of renewable energy resources. In Hong Kong, the government has also recognized the importance of promoting the use of renewable energy resources. In 2008, the government of Hong Kong [1] sets a target of generating between 1% and 2% of Hong Kong's total electricity supply from renewable energy sources by 2012.

According to the Hong Kong annual report of 2009 [2], buildings took up about 89% of total electricity consumption in Hong Kong. Reducing electricity consumption of buildings is instrumental in reducing greenhouse gas emissions and relieving energy crisis. Because the weather of Hong Kong is the typical humid subtropical climate, air conditioning contributes a significant percentage of the total energy consumption of buildings in Hong Kong. According to Hong Kong energy end-use data 2010 [3], about 24% of commercial energy end-use and 20% of residential energy end-use were consumed for air conditioning.

Building-integrated photovoltaic (BIPV) is a PV application close to being capable of delivering electricity at less than the cost of grid electricity to end users in certain peak demand niche markets [4]. Compared with PV systems, one of important advantages of BIPV systems is that PV modules can replace conventional building materials. The savings in the purchase and installation of conventional materials can lower the net cost of BIPV systems. PV modules provide fully integrated electricity generation while also serve as part of the weather protective building envelopes. If BIPV systems are properly designed, the cooling load of building envelopes which PV modules are integrated into can also be eliminated. Apart from the electricity generation of PV modules, the cooling energy consumption reduction due to cooling load reduction of building envelopes should also be regarded as parts of the total electricity saving when the energy performance of BIPV systems is evaluated.

In recent years, many theoretical and experimental studies have been conducted to maximize the energy benefits of BIPV systems, in terms of the power output of PV modules and the cooling load reduction of buildings. Chow et al. [5,6] has evaluated and tested a southwest-facing PVT wall located in Hong Kong. In comparison with the conventional wall, the range of the PVT wall internal surface temperature is smaller and the space cooling load can be lowered by 50% in the hottest summer. Zogou et al. [7] has examined south-facing double PV facades of an office building on basis of energy simulation using TRNSYS. The existence of double PV facades can considerably reduce the cooling energy consumption of buildings if alternative night cooling strategy is allowed. Wang et al. [8] indicated that a BIPV roof with ventilated air gap has high PV energy efficiency and low cooling load in hot summer. James et al. [9] investigated a semitransparent PV atrium and found that it has a great amount of multiple advantages such as electricity gen-

* Corresponding author. Tel.: +852 2766 4559.
E-mail address: 07901289r@polyu.edu.hk (L. Sun).

0306-2619/$ - see front matter © 2011 Elsevier Ltd. All rights reserved.
doi:10.1016/j.apenergy.2011.01.062

Nomenclature

P_{pv}	power output of PV module (W/m^2)
G_{pv}	solar radiation absorbed by PV module (W/m^2)
G_{wall}	solar radiation absorbed by concrete wall (W/m^2)
G_{window}	solar radiation absorbed by window (W/m^2)
G_{bw}	beam solar radiation absorbed by window (W/m^2)
G_{dw}	diffuse solar radiation absorbed by window (W/m^2)
G_{rw}	ground reflected solar radiation absorbed by window (W/m^2)
G_{tt}	total solar radiation of tilt surface (W/m^2)
G_{bt}	beam solar radiation of tilt surface (W/m^2)
G_{dt}	diffuse solar radiation of tilt surface (W/m^2)
G_{grt}	ground reflected solar radiation of tilt surface (W/m^2)
G_{bh}	beam solar radiation of horizontal surface (W/m^2)
G_{dh}	diffuse solar radiation of horizontal surface (W/m^2)
R_b	geometric factor (–)
T_{ao}	outdoor air temperature (K)
T_{ai}	indoor air temperature (K)
T_e	solar-air temperature (K)
F_1, F_2	brightness coefficient (–)
F_{r-o}	view factor from overhang to sky (–)
F_u	unshaded ratio (–)
Q_c	conductive and convective heat gain (W)
Q_s	solar heat gain (W)
U_{window}	overall heat transfer coefficient of window (W/m^2)
U_{wall}	overall heat transfer coefficient of concrete wall (W/m^2)
A_{window}	area of window (m^2)
A_{wall}	area of concrete wall (m^2)
h_o	outside convective heat transfer coefficient (W/m^2 K)
h_i	inside convective heat transfer coefficient (W/m^2 K)
v	wind velocity (m/s)
R	wall utilization fraction (%)

Greek letters

θ	incidence angle of beam solar radiation (°)
β	tilt angle (°)
ρ	ground reflectance (–)
φ	incidence angle of wind (°)
α	absorptance (–)
τ	transmittance (–)
ε	emittance (–)

Indices

pv	photovoltaic module
o	outdoor
i	indoor
b	beam
d	diffuse
gr	ground reflected
h	horizontal
t	tilt

eration, solar shading, attractive look and environmental statements. Yoo et al. [10,11] examined a south-facing shading-type BIPV system and suggested that the shading-type BIPV claddings should be applied for both generating electricity and providing shading for the building. The present author [12] has also discussed the effect of south-facing shading-type BIPV claddings on the cooling load reduction of windows.

The performance of BIPV systems is highly influenced by the orientations of PV modules [13]. There is little available information about the effect of surface azimuth angles on the energy performance of the shading-type BIPV claddings. This paper aims to investigate the combined energy effect produced by the shading-type BIPV claddings, including the power output of PV modules, the electricity consumption reduction caused by the cooling load reduction of windows and concrete walls. The optimum tilt angles of the shading-type BIPV claddings at different orientations are found out to provide the most desirable energy saving effect. These simulation results are illustrated graphically for references of engineers or designers.

2. Electricity generated by PV modules

2.1. Power model of PV modules

The power output of crystalline silicon PV modules mainly depends on the outdoor air temperature and the total solar radiation absorbed by PV modules. One simplified applicable model developed by Lu et al. [14] for the maximum power output of PV modules is utilized in this paper. The model and regressed parameters are described as follows

$$P_{pv}(t) = -(a_1 G_{pv}(t) + a_2)(T_{ao}(t) + 0.03375 G_{pv}(t)) + a_3 G_{pv}(t) + a_4 \quad (1)$$

where P_{pv} is the power output of PV modules. G_{pv} is the total solar radiation absorbed by PV modules. T_{ao} is the outdoor air temperature. a_1, a_2, a_3, and a_4 are constants from regression results for PV modules and can be obtained from site tests.

2.2. Total solar radiation absorbed by PV modules

PV modules can be installed at any surface azimuth angles and tilt angles. The total solar radiation absorbed by PV modules is the sum of the beam solar radiation, diffuse solar radiation and ground reflected solar radiation and is expressed as follows

$$G_{pv}(t) = G_{bt}(t) + G_{dt}(t) + G_{grt}(t) \quad (2)$$

The beam part can be simulated by

$$G_{bt}(t) = G_{bh}(t)\frac{\cos\theta_t}{\cos\theta_h} = G_{bh}(t)R_b \quad (3)$$

where θ_h is the incidence angle of the beam solar radiation on a horizontal surface and θ_t is that of a tilt surface. G_{bh} and G_{dh} are respectively the beam solar radiation and diffuse solar radiation incident on a horizontal surface. R_b is the geometric factor.

The Perez model [15] is utilized to evaluate the diffuse solar radiation as below

$$G_{dt}(t) = G_{dh}(t)\left(\cos^2\left(\frac{\beta}{2}\right)(1-F_1) + F_1\left(\frac{f_1}{f_2}\right) + F_2\sin(\beta)\right) \quad (4)$$

where β is the tilt angle of PV modules. F_1 and F_2 are brightness coefficients and functions of sky clearness (ε) and sky brightness (Δ). The value of f_1/f_2 determines the angular location of the circumsolar region.

The ground reflected solar radiation is expressed as

$$G_{grt}(t) = (G_{bh}(t) + G_{dh}(t))\rho\frac{1-\cos\beta}{2} \quad (5)$$

where ρ is the ground reflectance. If there is snow on the ground, the range of ρ is from 0.35 to 0.6. If there is no snow on the ground, ρ is about 0.2, which is a nominal value for green vegetation and some soil types.

3. Cooling load of windows and concrete walls

The radiant time series (RTS) method [16] is utilized to calculate the cooling load of windows and concrete walls. The RTS method is a new simplified method for performing cooling load calculations that is derived from the heat balance (HB) method and can quantify each component contribution to the total cooling load.

3.1. Solar radiation absorbed by windows

The total solar radiation absorbed by windows can be expressed as

$$G_{window}(t) = G_{bh}(t)R_b + G_{dh}(t)\left(\frac{1-F_1}{2} + F_1\left(\frac{f_1}{f_2}\right) + F_2\right) + 0.5(G_{bh}(t) + G_{dh}(t))\rho \quad (6)$$

It is known that the most significant effect of overhangs is to intercept the beam solar radiation from the sun before it reaches windows. At the same time, the diffuse solar radiation received by windows can also be affected by overhangs. Thus, the total solar radiation absorbed by windows with overhangs is described as

$$G'_{window}(t) = G_{bh}(t)R_bF_u(t) + G_{dh}(t)\left[\left(\frac{1-F_1}{2} + F_1\left(\frac{f_1}{f_2}\right) + F_2\right) - F_{r-o}\right] + 0.5(G_{bh}(t) + G_{dh}(t))\rho \quad (7)$$

where F_{r-o} is the view factor from overhangs to the sky and determined by the geometry and relative position of windows and overhangs [17]. F_u is the ratio of the beam solar radiation received by a partly shaded window to the beam solar radiation received by an unshaded window. The value of F_u not only depends on the dimensions of overhangs and windows but also depends on the incidence angle of the beam solar radiation. The value of F_u can be calculated by the models proposed by Sun et al. [12].

3.2. Heat gain of windows

The total heat gain of windows consists of three parts as follows:

(1) the conductive and convective heat gain caused by the temperature difference between the outdoor and indoor air;
(2) the net long-wave radiant heat gain between windows and their surroundings;
(3) the short-wave solar radiant heat gain from the sun.

It is supposed that the sky, ground, surrounding objects and windows have the same temperature. With this assumption, the net long-wave radiant heat gain between windows and their surroundings can be regarded as zero.

Heat gain caused by the conductive and convective heat transfer is described as

$$Q_c(t) = U_{window}A_{window}(T_{ao}(t) - T_{ai}(t)) \quad (8)$$

where U_{window} and A_{window} are the overall heat transfer coefficient and area of windows. T_{ai} is the indoor air temperature.

The amount of solar heat gain due to the short-wave solar radiation incident on windows is usually determined in terms of solar heat gain factors (SHGF). In this paper, an applicable model developed by Powell et al. [18] is utilized to estimate the solar heat gain and is expressed as below

$$Q_s(t) = G_{bw}(t)(\tau_b + \alpha_bN_i) + (G_{dw}(t) + G_{grw}(t))(\tau_d + \alpha_dN_i) \quad (9)$$

N_i is the inward-flowing fraction of the absorbed solar radiation and its value can be calculated using the following models [19]

$$N_i = \frac{h_i}{h_i + h_o} \quad (10)$$

$$h_o = 16.21v_w^{0.452} \quad (11)$$

$$v_w = 0.68v_o - 0.5(20^\circ \leqslant \varphi \leqslant 160^\circ) \quad (12)$$

$$v_w = 0.157v_o - 0.027(\varphi < 20^\circ \text{ or } \varphi > 160^\circ) \quad (13)$$

where φ is the incidence angle of wind. v_w is the velocity of the wind blowing over the window outside surface. v_o is the wind velocity recorded by local observatory. h_i and h_o are the convective heat transfer coefficients respectively for the inside surface and outside surface. The value of h_i used in this paper is 8.29 W/(m^2 K), which is recommended by the ASHRAE hand book [16].

The transmittance and absorptance for the beam component depend on the incidence angle of the beam solar radiation. The correlations proposed by Stephenson [20] are used as follows

$$\tau_b = -0.00885 + 2.71235\cos\theta_w - 0.62062\cos^2\theta_w - 7.07329\cos^3\theta_w + 9.75995\cos^4\theta_w - 3.89922\cos^5\theta_w \quad (14)$$

$$\alpha_b = 0.001154 + 0.77674\cos\theta_w - 3.94657\cos^2\theta_w + 8.57881\cos^3\theta_w - 8.38135\cos^4\theta_w + 3.01188\cos^5\theta_w \quad (15)$$

For the diffuse and ground reflected solar radiation, the values of τ_d and α_d used in this paper are 0.799 and 0.0544 respectively [20].

3.3. Heat gain of concrete walls

The conductive heat input of concrete walls is expressed by the familiar conduction equation as

$$Q_{wall}(t) = U_{wall}A_{wall}(T_e(t) - T_{ai}(t)) \quad (16)$$

where U_{wall} and A_{wall} are the overall heat transfer coefficient and area of concrete walls. T_e is the solar-air temperature and is defined as [16]

$$T_e(t) = T_{ao}(t) + \frac{\alpha_{wall}G_{wall}(t)}{h_o} - \frac{\varepsilon_{wall}\Delta R}{h_o} \quad (17)$$

where α_{wall} and ε_{wall} are the absorptance and hemispherical emittance of concrete walls. ΔR is the difference between the long-wave radiation emitted by the blackbody at the outdoor air temperature and the long-wave radiation incident on concrete walls from the sky and surrounding objects.

According to ASHRAE hand book [16], it is common practice to assume $\varepsilon_{wall} \cdot \Delta R = 0$ for vertical surfaces. And it is appropriate for a light color concrete wall surface that the value of α_{wall}/h_o equals 0.15. Therefore, the expression of the solar-air temperature can be simplified as

$$T_e(t) = T_{ao}(t) + 0.15G_{wall}(t) \quad (18)$$

4. Simulation prerequisites

Fig. 1 shows the schematic of the shading-type BIPV claddings. PV modules are installed on concrete walls between two adjacent windows. The dimension of windows is 4.5 m × 1.5 m. The height of concrete walls is 1.7 m. The ratio of the height of concrete walls installed with PV modules to the total height of concrete walls is defined as the wall utilization fraction (R). In this paper, wall utilization fractions are varied from 20% to 100% at 20% increment.

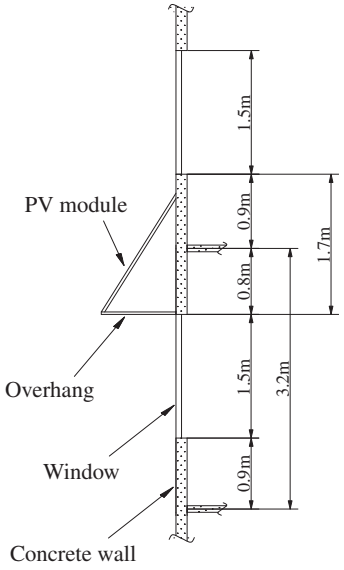

Fig. 1. The schematic of the shading-type BIPV claddings.

Table 1
Length of overhangs.

Length of overhangs	Wall utilization fraction				
Tilt angle (°)	20%	40%	60%	80%	100%
20	0.93 m				
30	0.59 m	1.18 m			
40	0.41 m	0.81 m	1.22 m		
50	0.29 m	0.57 m	0.86 m	1.14 m	1.43 m
60	0.20 m	0.39 m	0.59 m	0.78 m	0.98 m
70	0.12 m	0.25 m	0.37 m	0.50 m	0.62 m
80	0.06 m	0.12 m	0.18 m	0.24 m	0.30 m

A maximum length of 1.5 m for the overhang is adopted because it is the maximum projection from an external wall that can be exempted from the gross floor area and site coverage calculation [21]. Thus different tilt angles were selected for different wall utilized fractions to make the overhang length be smaller than 1.5 m. Table 1 lists different values of the overhang length for different wall utilization fractions and tilt angles.

5. Simulation results and discussions

The annual simulation of the energy performance of shading-type BIPV claddings is conducted on basis of the hourly TMY weather data of Hong Kong [22]. Each contribution of the total electricity saving of shading-type BIPV claddings, such as PV electricity generation, window cooling load reduction and concrete wall cooling load reduction, has been analyzed.

5.1. Annual electricity generation of PV modules

Fig. 2 shows the annual electricity generation per unit PV area for different surface azimuth angles. The maximum electricity generation of 76.7 kW h/m^2 occurs when PV modules are installed on south-facing facades at the tilt angle of 10°. If the east-facing PV modules have to be installed vertically, the annual electricity generation is 43.2 kW h/m^2, decreased by 43.8% compared with the maximum value. In general, PV modules produce more electricity annually at smaller tilt angles than at larger ones. The annual electricity generation of PV modules decreases sharply when tilt angles exceed 40°. When tilt angles are smaller than 60°, the ascending order of annual electricity generation is −90°, −45°, 90°, 45° and 0°. In contrary, the ascending order of annual electricity generation becomes −90°, −45°, 90°, 0° and 45°. Thus, the orientations of south and southwest are two better choices for PV module installation. The optimum tilt angles of PV modules are 10° for both south and southwest facades.

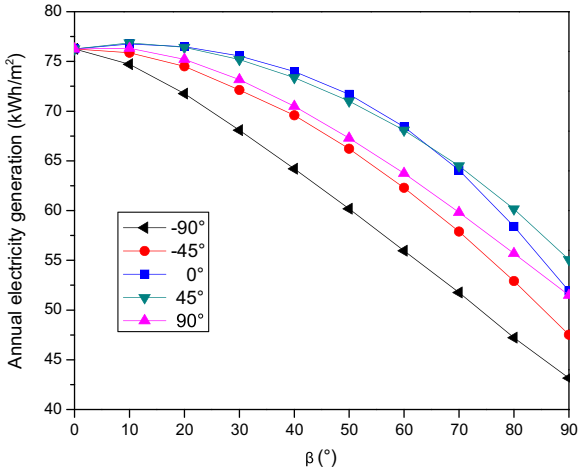

Fig. 2. Annual electricity generation per unit PV area.

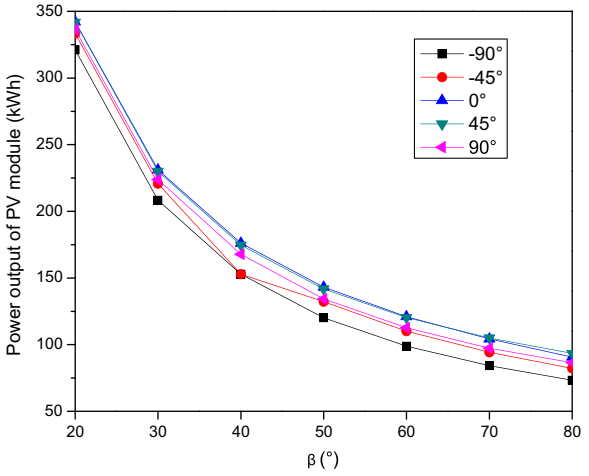

Fig. 3. Annual power output of PV modules (R = 20%).

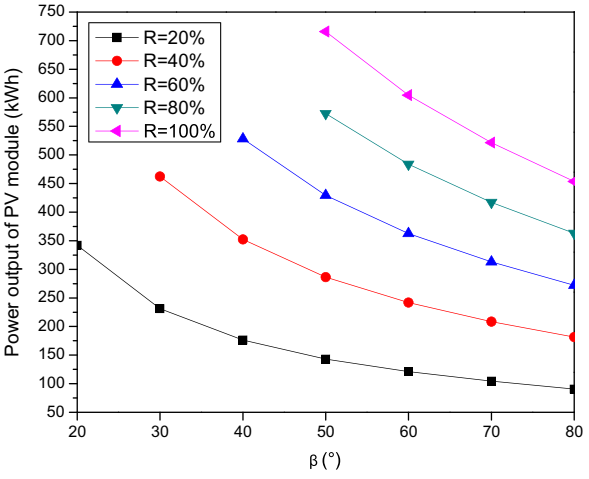

Fig. 4. Annual power output of south-facing PV modules.

Figs. 3 and 4 present the annual power output of PV modules for different orientations and wall utilization fractions. In comparison of Figs. 3 and 4, it is concluded that wall utilization fractions have more significant effect on the power output of PV modules than that of surface azimuth angles. As indicated in Fig. 4, south-facing PV modules can produce the maximum power output of 715.7 kW h with the tilt angle of 50° and the wall utilization fraction of 100%. Correspondingly, the overhang length is 1.43 m, which is also the biggest overhang length used in this paper.

5.2. Annual cooling load reduction ratio of windows and concrete walls

As shown in Figs. 5 and 6, the variations of cooling load per unit area of windows and concrete walls have the same trend when surface azimuth angles change from −90° to 90°. Both southwest-facing windows and concrete walls can lead to more cooling load than other orientations. It can also be inferred that the annual cooling load of concrete walls can be neglected compared with that of windows.

Figs. 7 and 8 present the annual cooling load reduction and cooling load reduction ratio of widows when the wall utilization fraction is 20%. It can be observed from Fig. 7 that the cooling load reduction of southwest-facing windows is the largest, while that of east-facing windows is the smallest. As illustrated in Fig. 8, there is

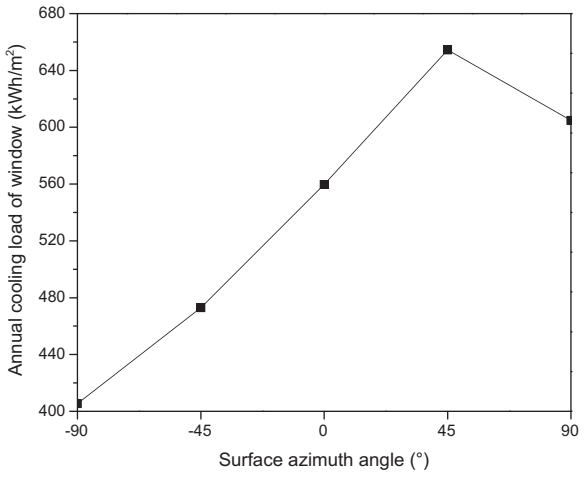

Fig. 5. Annual cooling load per unit window area.

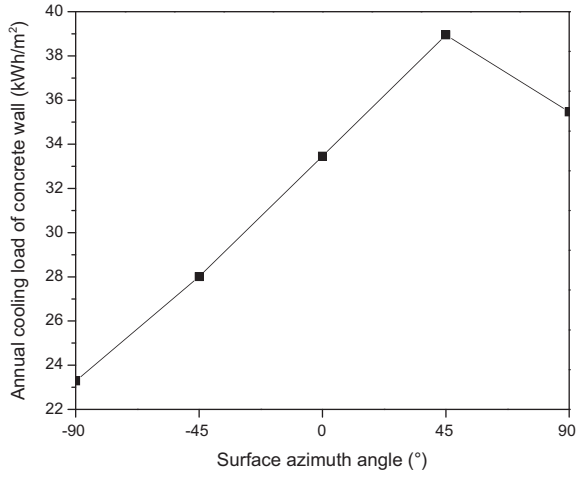

Fig. 6. Annual cooling load per unit concrete wall area.

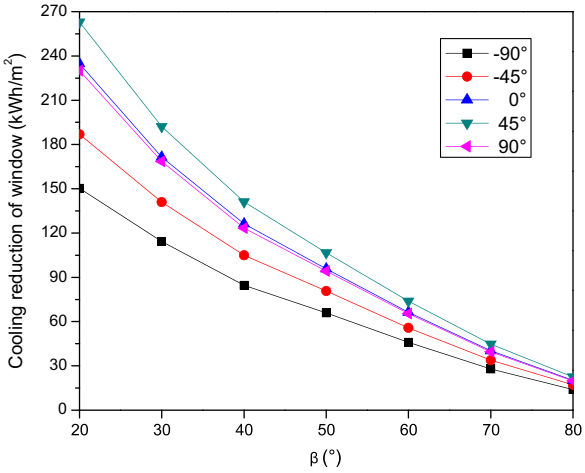

Fig. 7. Cooling load reduction per unit window area (R = 20%).

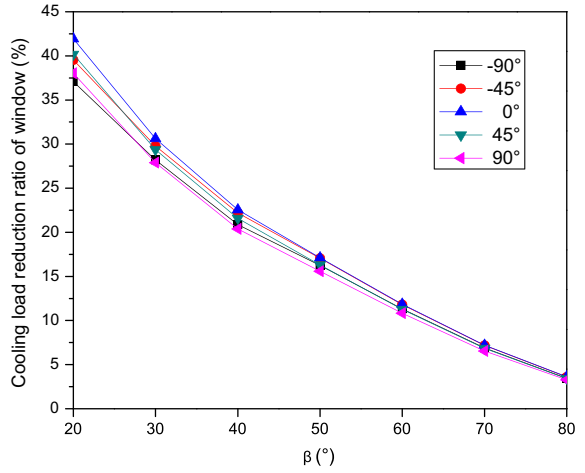

Fig. 8. Cooling load reduction ratio of windows (R = 20%).

no significant difference among the window cooling load reduction ratios of all five orientations, particularly at the larger tilt angles. In addition, south-facing windows have larger cooling load reduction ratio than other orientations.

Fig. 9 shows the annual cooling load reduction ratio of south widows. It can be seen that when wall utilization fractions increase from 20% to 100%, the cooling load reduction ratio increase and growth rates decrease as wall utilization fractions become larger. The cooling load reduction ratio is as high as 51.6% when the tilt angle equals 50° and the wall utilization fraction is 100%. While tilt angles increase to 80°, the cooling load reduction ratio decreases to 17.8%. Thus, the shading-type BIPV claddings with small tilt angles are more effective for window cooling load reduction. In addition, the effect of tilt angles on window cooling load reduction ratio is more significant than that of surface azimuth angles.

In comparison of Figs. 6 and 10, it is can be seen that the cooling load and the cooling load reduction of concrete walls have the same variation trend and can reach their maximum values when the surface azimuth angle equals 45°. Fig. 11 shows that the annual cooling load reduction ratios of concrete walls are very large. The minimum value of cooling load reduction ratios is 37.1%, while the maximum value is as high as 243.2%. When wall utilization fractions are lager than 60%, the cooling load reduction ratios of concrete walls are all bigger than 100%. In addition, it is indicated that the ascending order of annual cooling load reduction ratio of concrete walls is 45°, 90°, 0°, −45° and −90°.

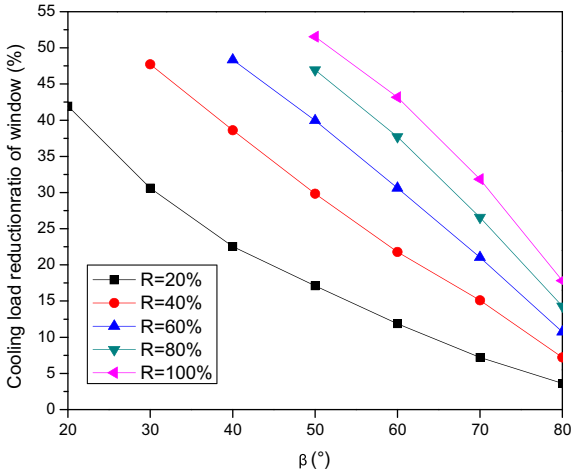

Fig. 9. Cooling load reduction ratio of south windows.

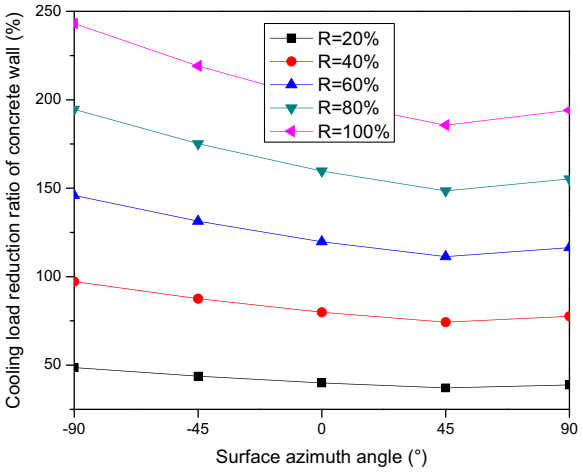

Fig. 11. Cooling load reduction ratio of concrete walls.

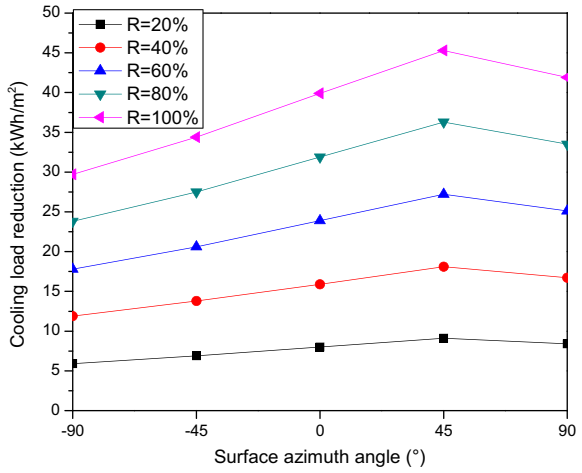

Fig. 10. Cooling load reduction per unit concrete wall area.

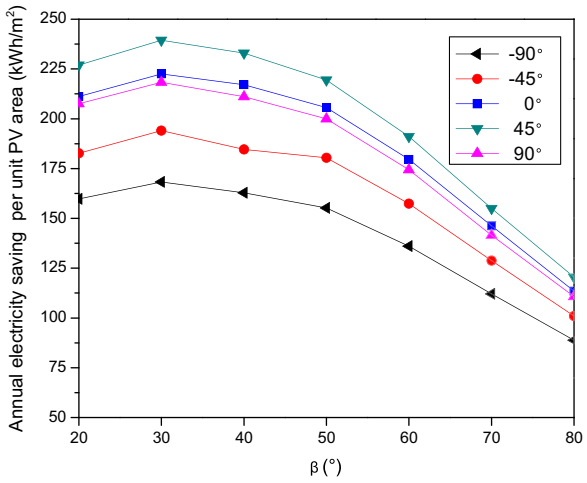

Fig. 12. Annual electricity saving per unit PV area ($R = 20\%$).

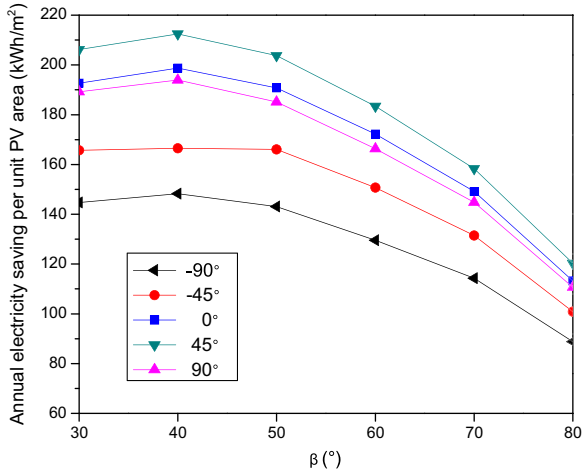

Fig. 13. Annual electricity saving per unit PV area ($R = 40\%$).

5.3. Combined effects of electricity generation and cooling load reduction

As mentioned above, the annual electricity generation and cooling load reduction produced by the shading-type BIPV claddings contribute to the total electricity saving of buildings. It is necessary to analyze the combined effects of these two contributions and to evaluate the optimum position of the shading-type BIPV claddings so that the maximum electricity saving is achieved. By using the COP of the HVAC system, the cooling load reduction of windows and concrete walls can be converted into the corresponding electricity consumption reduction. Supposing that the building is cooled by an air cooled HVAC system, the value of COP is set to be 2.8 [23]. Thus, the total electricity saving of the shading-type BIPV claddings at different orientations can be determined.

Since the initial cost of PV modules is high, annual electricity saving per unit PV area is utilized to evaluate the energy performance of the shading-type BIPV claddings. Figs. 12–16 show the simulation results of annual electricity saving with different wall utilization fractions and orientations. In comparison of Figs. 12–16, it is seen that as wall utilization fractions increase, the amount of annual electricity saving produced by the shading-type BIPV claddings decreases. When wall utilization fraction are smaller, such as 20%, 40% and 60%, the maximum annual electricity saving does not occur at the smallest tilt angle. While wall utilization fractions are larger, such as 80% and 100%, PV modules at smaller tilt angles can produce more electricity saving than that of larger ones. Table 2 summarizes these optimum tilt angles for different orientations and wall utilization fractions.

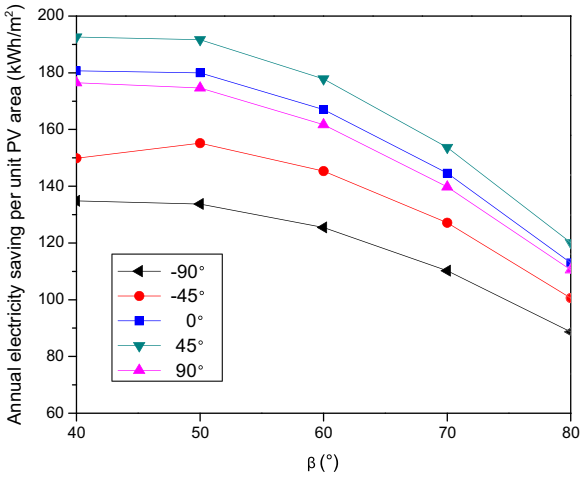

Fig. 14. Annual electricity saving per unit PV area (R = 60%).

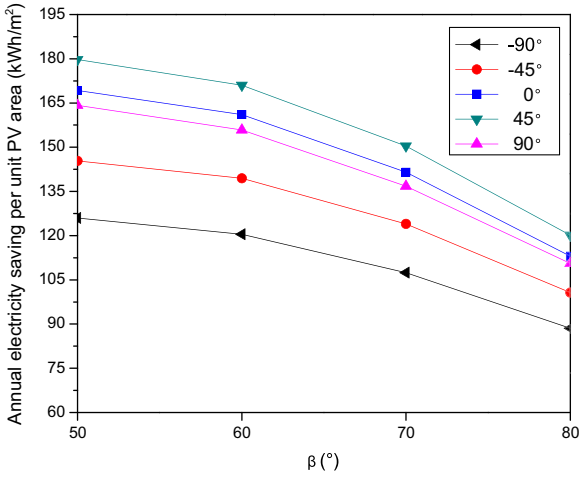

Fig. 15. Annual electricity saving per unit PV area (R = 80%).

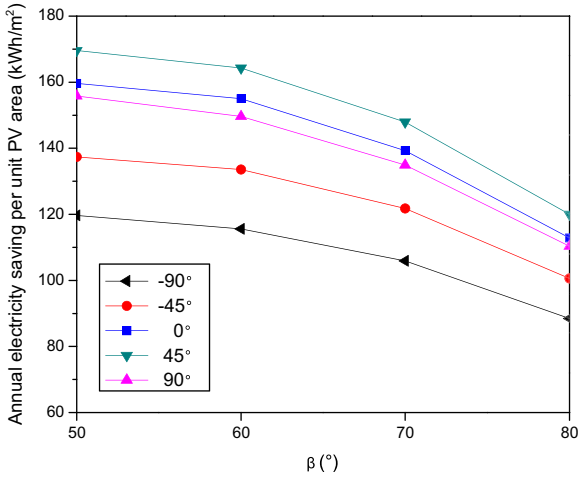

Fig. 16. Annual electricity saving per unit PV area (R = 100%).

It is observed from the curves that the southwest-facing BIPV claddings can obtain more electricity saving than that of other orientations. The maximum electricity saving per unit PV area of 239.5 kW h/m^2 occurs when the shading-type BIPV claddings have the surface azimuth angle of 45°, the tilt angle of 30° and the wall utilization fraction of 20%. The east-facing BIPV claddings with the tilt angle of 80° and the wall utilization fraction of 100% produce the minimum electricity saving of 88.5 kW h/m^2, lowered by 63% compared with the maximum value. In addiction, the maximum electricity saving per unit PV area is twice more than the maximum electricity generation of PV modules. The shading-type BIPV systems can produce much more energy benefits than that of PV systems.

Table 2
Optimum tilt angles for different orientations and wall utilization fractions.

Optimum tilt angle	Wall utilization fraction				
Surface azimuth angle (°)	20%	40%	60%	80%	100%
−90	30°	40°	40°	50°	50°
−45	30°	40°	50°	50°	50°
0	30°	40°	40°	50°	50°
45	30°	40°	40°	50°	50°
90	30°	40°	40°	50°	50°

6. Conclusions

In this paper, the impact of building orientations, inclinations and wall utilization fractions on the energy performance of the shading-type BIPV claddings is discussed in terms of annual power output of PV modules and cooling load reduction of windows and concrete walls. Some specific findings from this case study are described as follows:

(1) If the annual electricity generation per unit PV area is concerned, the orientations of south and southwest are two better choices for PV module installation for the weather in Hong Kong. The maximum electricity generation per unit PV area is 76.8 kW h/m^2 when the PV modules are installed on south façades at the tilt angle of 10°.
(2) The shading-type BIPV claddings have significant effect on cooling load reduction of windows and concrete walls. The maximum cooling load reduction ratios are 51.6% and 243.2% respectively for windows and concrete walls.
(3) When the area of PV modules is considered, the maximum electricity saving of the shading-type BIPV claddings is 239.5 kW h/m^2, which is twice more than the maximum electricity generation of the PV modules.
(4) Different optimum tilt angles of the shading-type BIPV claddings are obtained for different orientations and wall utilization fractions. In this case study, the optimum tilt angles for different designs vary from 30° to 50°. When installed with smaller wall utilization fractions, the shading-type BIPV claddings are more cost-effective than that with larger wall utilization fractions.

The simulation results indicate that the shading-type BIPV claddings can significantly increase the total energy benefits relative to PV modules. It is thus a good choice to apply the shading-type BIPV system in buildings of Hong Kong. In addition, these simulation results are good references for the design of integrating PV modules into buildings.

Acknowledgment

The work described in this paper was supported by a grant from the Guangdong – Hong Kong Technology Cooperation Funding Scheme (TCFS).

References

[1] Sustainable development unit office of chief secretary for administration. A first sustainable development strategy for Hong Kong. Hong Kong Special Administrative Region; 2008.

[2] The information services department. The Hong Kong annual report of 2009. Hong Kong Special Administrative Region; 2009.

[3] Electrical and mechanical services department. Hong Kong energy end-use data 2010. Hong Kong Special Administrative Region; 2010.

[4] Norton B, Eames PC, Mallick TK, Huang MJ, McCormack SJ, Mondol JD, et al. Enhancing the performance of building integrated photovoltaics. Solar Energy. doi:10.1016/j.solener.2009.10.004.

[5] Chow TT, He W, Ji J. An experimental study of facade-integrated photovoltaic/water heating system. Appl Therm Eng 2007;27:37–45.

[6] Chow TT, Chan ALS, Fong KF, Lin Z, Ji J. Annual performance of building-integrated photovoltaic water-heating system for warm climate application. Appl Energy 2009;86:689–96.

[7] Zogou O, Stapountzis H. Energy analysis of an improved concept of integrated PV panels in an office building in central Greece. Appl Energy 2011;88:853–66.

[8] Wang YP, Tian W, Ren JB, Zhu L, Wang QZ. Influence of a building's integrated-photovoltaics on heating and cooling loads. Appl Energy 2006;83(9):989–1003.

[9] James PAB, Jentsch MF, Bahaj AS. Quantifying the added value of BiPV as a shading solution in atria. Solar Energy 2009;83:220–31.

[10] Yoo SH, Lee ET. Efficiency characteristic of building integrated photovoltaics as a shading device. Build Environ 2002;37:615–23.

[11] Yoo SH, Manz H. Available remodeling simulation for a BIPV as a shading device. Solar Energy Mater Solar Cells 2011;95(1):394–7.

[12] Sun LL, Yang HX. Impacts of the shading-type building-integrated photovoltaic claddings on electricity generation and cooling load component through shaded windows. Energy Build 2010;42(4):455–60.

[13] Yang HX, Lu L. The optimum tilt angles and orientations of PV claddings for building-integrated photovoltaic (BIPV) applications. J Solar Energy Eng 2007;129:253–5.

[14] Lu L, Yang HX. A study on simulations of the power output and practical models for building integrated photovoltaic systems. J Solar Energy Eng 2004;126:929–35.

[15] Perez R, Ineichen P, Seals R. Modelling of daylight availability and irradiance components from direct and global irradiance. Solar Energy 1990;44:271–89.

[16] American society of heating, refrigerating and air conditioning engineers. ASHARE handbook-fundamentals. Atlanta: ASHARE Inc.; 2009.

[17] Utzinger DM, Klein SA. A method of estimating monthly average solar radiation on shaded receivers. Solar Energy 1979;23:369–78.

[18] Powell GL, Yellott JI. Solar heat gain factors on average days. In: Proceeding of American section of the international solar energy society annual meeting; 1980. p. 826–30.

[19] Loveday DL, Taki AH. Convective heat transfer coefficients at a plane surface on a full-scale building façade. Int J Heat Mass Trans 1996;39(8):1729–42.

[20] Stephenson DG. Equations for solar heat gain through windows. Solar Energy 1965;9(2):81–6.

[21] Hong Kong building department. Joint practice note no. 1 – incentives for green buildings. Hong Kong Special Administrative Region; 2001.

[22] Lu L, Yang HX. Study on typical meteorological years and their effect on building energy and renewable energy simulations. ASHARE Trans 2004;110(2):424–31.

[23] Yik FWH, Burnett J, Prescott I. Predicting air-conditioning energy consumption of a group of buildings using different heat rejection methods. Energy Build 2001;33:151–66.